Quantification of pathway crosstalk reveals novel synergistic drug combinations for breast cancer

Samira Jaeger[1], Ana Igea[1], Rodrigo Arroyo[1], Victor Alcalde[1], Begoña Canovas[1], Modesto Orozco[1, 2], Angel R. Nebreda[1, 3] and Patrick Aloy[1, 3*]

[1] Institute for Research in Biomedicine (IRB Barcelona). The Barcelona Institute of Science and Technology. c/ Baldiri i Reixac 10-12. 08028 Barcelona, Catalonia, Spain

[2] Department of Biochemistry and Molecular Biology, University of Barcelona. 08028 Barcelona, Catalonia, Spain

[3] Institució Catalana de Recerca i Estudis Avançats (ICREA). Pg. Lluís Companys 23. 08010 Barcelona, Catalonia, Spain

Running title: Network analysis identifies drug synergies

Key words: Breast cancer / drug synergies / network biology / pathway crosstalk analysis

Financial support of each author: This work was partially supported by the Spanish Ministerio de Ciencia e Innovación (BIO2010-22073 and BFU2010-17850), the European Commission (Agreement nº: 306240) and the European Research Council (Agreements nº: 614944 and 294665) awarded to P. Aloy and

A.R. Nebreda. IRB Barcelona and the EU Marie Curie Actions COFUND program support S. Jaeger. A.R. Nebreda is supported by the Fundación BBVA.

* Corresponding author:

Patrick Aloy. Tel: +34 934039690; Email: patrick.aloy@irbbarcelona.org

Conflict of interest: The authors declare no conflict of interest.

Total word count: 4,994

Total number of figures and tables: 7

Abstract

Combinatorial therapeutic approaches are an imperative to improve cancer treatment, since it is critical to impede compensatory signaling mechanisms that can engender drug resistance to individual targeted drugs. Currently approved drug combinations result largely from empirical clinical experience and cover only a small fraction of a vast therapeutic space. Here we present a computational network biology approach, based on pathway crosstalk inhibition, to discover new synergistic drug combinations for breast cancer treatment. In silico analysis identified 390 novel anti-cancer drug pairs belonging to 10 drug classes that are likely to diminish pathway crosstalk and

display synergistic anti-tumor effects. Ten novel drug combinations were validated experimentally, and seven of these exhibited synergy in human breast cancer cell lines. In particular, we found that one novel combination, pairing the estrogen response modifier raloxifene with the c-Met/VEGFR2 kinase inhibitor cabozantinib, dramatically potentiated the drugs' individual anti-tumor effects in a mouse model of breast cancer. When compared to high-throughput combinatorial studies without computational prioritization, our approach offers a significant advance capable of uncovering broad-spectrum utility across many cancer types.

Introduction

Breast cancer is a very heterogeneous disease regarding the underlying molecular alterations, the cellular composition of tumors, and the different clinical outcomes (1), which hampers the design of effective treatment strategies (2). To account for this intrinsic diversity, drug discovery efforts have shifted towards mechanism-based and target-oriented strategies, particularly aiming at modulating specific molecular pathways, patient-specific genetic alterations and the tumor microenvironment (3,4).

Despite the expanding repertoire of new anti-cancer agents, treatment failure remains a major challenge in the management of most advanced solid cancers, including breast cancer (5,6). Multiple compensatory mechanisms are known to counterbalance therapeutic effects, eventually leading to treatment failure (6). One of the most promising strategies for better clinical outcomes is the use of combinatorial therapy to target the distinct adaptive response mechanisms (7,8), which may also help to overcome toxicity associated with higher doses of single drugs. In addition, synergistic drug combinations are often more specific and therefore improve the therapeutically relevant selectivity (9). However, although becoming the standard care in (breast) cancer treatment, most approved drug

combinations are the result of empirical clinical experience, and often rely on similar mechanisms of action as pre-existing drug combinations, which prevented a systematic sampling of the therapeutic space (Supplemental Fig. S1).

Identifying drug combinations with therapeutic effect remains a challenging task given the exhaustive number of possibilities. Different approaches are available for predicting drug combinations for complex diseases, mostly including mathematical modeling, stochastic search techniques, as well as cell context-based methods like global gene expression or targeted phospho-proteomics profiling (10-13). More recently, network-based models have been proposed for identifying drug synergies and for examining the mechanisms of action of efficient combinations (14-16).

Experimental studies have shown that cancer cells are able to adapt signaling pathway circuits upon drug treatment by establishing alternative signaling routes through crosstalk (17,18). Hence, a critical aspect to improve cancer treatment is not only to inhibit the primary oncogenic pathways that induce abnormal cell proliferation but, simultaneously, to prevent functional redundancies and pathway crosstalk that facilitate survival of cancer cell

populations rendering tumors resistant to therapy. Current network pharmacology principles aim for a synergistic multi-target intervention strategy to improve clinical efficacies, while tackling critical aspects such as drug resistance (19,20). In line with this idea, we have derived a network-based computational method to quantify the crosstalk between signaling pathways involved in breast cancer and we assessed how combinatorial perturbations impact the signaling crosstalk. We then applied this measure to a set of approved and experimental breast cancer drugs to identify combinations, which could efficiently diminish pathway crosstalk and thereby increase clinical efficacy. Finally, we experimentally validated novel drug combinations in several human breast cancer cell lines and confirmed the *in vivo* synergistic effect between two drugs in mouse xenografts, emphasizing the potential clinical relevance of our strategy.

Material and Methods

Breast cancer drugs

We compiled a comprehensive set of drugs that are either prescribed or in clinical trials for breast cancer treatment. Primary information on FDA-approved breast cancer drugs has been gathered from the National Cancer Institute (NCI). This data has been complemented with information from DrugBank 3.0 (21) and the therapeutic targets database TTD (22). Overall, we collected 64 breast cancer agents of which 32 are approved. The number of experimental compounds used for breast cancer treatment is most likely higher; yet, the data is scattered across the literature, not accessible in an automatic manner and often there is no available information on the modulated therapeutic target(s).

Each drug has been associated with its therapeutic target(s). For drugs from DrugBank, we considered only primary targets. Only if none of the targets have a known pharmacological action we consider all targets for that drug. Targets from TTD were treated as primary therapeutic targets. We further extracted pathways and biological processes that are most likely modulated by a drug

through its target(s). Pathway information was retrieved from the KEGG database (23).

Depending on the mechanism of action, we divided drugs into cytotoxic and targeted agents. Furthermore, we classified the set of breast cancer drugs according to their therapeutic target(s) into 11 drug classes. The complete set of breast cancer drugs considered can be found in Supplemental Table S1.

Breast cancer drug combinations of clinical relevance

We extracted drug combinations considered for breast cancer therapy by mining the Drug combination database (DCDB) (24), the FDA orange book (25), the NCI and the ClinicalTrials.gov (26). In total, 170 drug combinations were obtained. Some of them are already approved while the majority is currently in clinical trials. Supplemental Fig. S1 provides an overview of the current drug combinations with respect to the 11 drug classes.

Therapeutic signaling networks and pathway crosstalk inhibition

To chart the therapeutic networks associated with each drug, we compiled all those KEGG pathways (excluding disease pathways) that include any of the primary targets of the drug. On average each drug affects 6.5 KEGG pathways

(median = 3, sd ± 8.3). Given the XML representation of a pathway, we created a directed network including proteins and their interactions whereas the type of an interaction, such as activation or inhibition, was used to determine the directionality of an edge in the network.

Based on the therapeutic signaling networks, we developed a crosstalk inhibition measure to estimate the amount of crosstalk signaling that can be prevented between pathways by inhibiting specific proteins simultaneously. The concept of pathway crosstalk refers to protein interactions shared between distinct pathways. Since these interactions might also influence the downstream signaling within a pathway, the concept also comprises proteins and interactions downstream of the respective crosstalking interactions (i.e. indirect crosstalk; Fig. 1).

Given two therapeutic signaling networks, we determined the potential crosstalk between them by identifying interactions directly and indirectly involved in the crosstalk, and representing them as a directed crosstalk network. Using this crosstalk representation, we then applied a topology-based measure, namely network efficiency (27), to determine the information flow within the network.

Network efficiency (NE) is defined as the sum of the inverse length of the shortest path between all network elements and can be computed as follows:

$$NE = \frac{\sum_{i \neq j} \frac{1}{d(i,j)}}{N(N-1)},$$

with *N* representing the number of network elements and *d* denoting the shortest distance between two elements i, j ∈ N. The network efficiency ranges between 0 and 1, where 1 indicates that all proteins communicate directly with each other, i.e., a fully connected network.

Using the network efficiency determined for crosstalking pathways, as described above, we simulated the inhibition of specific protein target(s) and measured the amount of signaling that persists (NE_X) when removing protein interactions affected by a pharmacological intervention. We determined the relative reduction of network efficiency, i.e., the pathway crosstalk inhibition (PCI), as follows:

$$PCI = 1 - \frac{NE_X}{NE}.$$

The final PCI for a given pair of breast cancer drugs is the average of the crosstalk inhibitions between each pair of crosstalking pathways forming the respective therapeutic networks.

Experimental validation of drug combinations

Drug combination experiments were conducted in five cell lines, four of them, namely MCF-7, MDA-MB-231, SKBR3 and BT474, representing distinct breast cancer subtypes. In addition, we also included U2OS, a bone osteosarcoma cell line, representing a widely used cancer cell line. When analyzing a combination, we tested the activity of the individual drugs D_1 and D_2, and the combination at four concentrations, selected from the literature to cover their activity range (Supplemental Table S2). To assess the cytostatic/cytotoxic effects of a single drug or a drug combination in cell lines, we employed the MTT assay for measuring cell viability (28).

Cells were seeded at 1,000 to 5,000 cells per well in 96-well flat-bottom cell culture plates. After 24 h of incubation at 37ºC with 5% CO_2, cells were exposed to four concentrations of drug or drug combinations for 72 or 120 h (Supplemental Table S2). Cell survival was determined using an MTT-based assay. All experiments were either performed in triplicates (individual drugs) or quadruplicates (drug combinations); repeated three independent times.

Further details on cell lines, culture conditions and drugs can be found in the Supplemental Information (Supplemental Section S1).

Drug combination index

Given the MTT cell viability measurements, we assessed whether a drug combination induces additive, synergistic or antagonistic effects in cultured cells. To this end, we determined the drug combination index (DCI) using the Loewe additivity as a reference model, assuming that a drug cannot interact with itself (29,30). This means that if two drugs are the same or very similar, we expect their combined effect at equal concentrations to be comparable to the one observed when administering one drug alone at double concentration.

The DCI of a combination is computed based on the half-maximal effective concentration that is needed to inhibit cell viability by X%, with X commonly corresponding to an inhibition level of 50% (i.e. IC_{50}). Formally, the DCI_X is defined as follows:

$$\mathrm{DCI_X} = \frac{\mathrm{C_{D1,X}}}{\mathrm{IC_{X,D_1}}} + \frac{\mathrm{C_{D2,X}}}{\mathrm{IC_{X,D_2}}}$$

$C_{D1,X}$ and $C_{D2,X}$ represent the concentration of drug D_1 and drug D_2 used in combination to induce an effect X while $IC_{X,D1}$ and $IC_{X,D2}$ indicate the corresponding concentrations of the single agents required to produce the same effect. In other words, the DCI measures the fractional shift between single

and combinatorial concentrations yielding an inhibition of cell survival of X%. The concept of the DCI is exemplified for one combination in Supplemental Fig. S2. Using this measure, we can quantify synergistic, additive and antagonistic combinatorial effects, commonly defined as DCI < 0.85, DCI ~1 and DCI > 1.2, respectively (Supplemental Table S3).

IC_X values can be determined from dose-response curves for any inhibition level *X*. Here, we used the *drc* R package to generate sigmoid-fitted dose-response curves from which we then estimated the IC_X for single drugs and combinations (31). In some cases the single agents do not reach the pre-defined inhibition level while in others the estimated IC_X corresponds to a value beyond the tested concentration range. In the latter one, we exploited the relative standard error (RSE) associated with each fit to decide whether to consider an IC_X (16). The influence of using different RSE thresholds for determining the DCI is discussed in Supplemental Section S2 and Table S4. No DCI is reported for cases where neither the single nor the combined inhibition induces the desired effect.

Dose reduction index

A major aim of synergistic drug combinations is to reduce the dose of a drug, thereby reducing toxicity while maintaining therapeutic efficacy. The dose

reduction index (DRI) measures to which extent the concentration of a drug in combination can be reduced at a given inhibition level X compared with the concentration of an individual drug alone.

$$\mathrm{DRI}_{\mathrm{X,D_1}} = \frac{\mathrm{IC}_{\mathrm{X,D_1}}}{\mathrm{C}_{\mathrm{D1,X}}}, \qquad \mathrm{DRI}_{\mathrm{X,D_2}} = \frac{\mathrm{IC}_{\mathrm{X,D_2}}}{\mathrm{C}_{\mathrm{D2,X}}}$$

In general, a DRI above 1 is considered to be beneficial. Furthermore, larger DRIs correlate with a larger magnitude of dose reduction for a given therapeutic effect.

Mouse xenograft model

MCF-7 human breast cancer cells were prepared in a 1:1 PBS:Matrigel (BD Biosciences) mixture and $1x10^6$ cells were injected directly into the mammary gland. When tumors reached a volume of 120-150 mm^3, mice were randomly assigned to different groups and treated for 15 days with cabozantinib (oral gavage, 2 mg/kg), raloxifene (i.p. 6 mg/kg), the combination of both (1 mg/kg of cabozantinib and 3 mg/kg of raloxifene), or the corresponding vehicles. At day 15, mice were sacrificed and tumors were formalin-fixed and paraffin-embedded. Sections were stained with haematoxylin and eosin (H&E), Ki67 (Novocastra) and the "In situ cell Death Detection Kit, Fluorescein" (Roche),

following manufacture' s instructions. Western blot analysis was used to measure the activity of selected proteins in tumor samples of the different groups. Further details can be found in the Supplemental Information (Section S3). For determining the statistical difference between the treatment groups we used the one-sided t-test.

Results

Pathway crosstalk inhibition (PCI) as a tool for inferring synergistic drug combinations

Alternative signaling through pathway crosstalk is one of the main mechanisms leading to treatment failure (18). Therefore, we devised a computational strategy to infer drug combinations that specifically addresses this problem. Our approach is based on the quantification of the level of crosstalk between signaling pathways that can be prevented by simultaneously inhibiting specific sets of proteins. The concept of pathway crosstalk refers to shared protein interactions between distinct signaling cascades, and the interactions downstream of the ones that crosstalk (Fig. 1). To determine pathway crosstalk

and inhibition, we first built the therapeutic networks associated with each individual drug by considering its set of known primary targets mapped onto well-annotated canonical pathways (23). We found that, on average, each drug can be associated with 6.5 signaling pathways, the sum of which constitutes its therapeutic signaling network. Interactions directly or indirectly (i.e. downstream) involved in crosstalk between drug pathways were integrated into a signaling network in which we then assessed the levels of crosstalk inhibition through individual or combinatorial target perturbations. Using a topology-based measure of network efficiency (27), we computed the flow of information within a crosstalk network before and after inhibiting individual or combined drug targets. Drug combinations with a high impact on PCI are expected to present promising drug combinations.

To examine the clinical relevance of the PCI for inferring novel drug combinations, we assessed its applicability on approved or tested breast cancer drug combinations. To this end, we generated all pairwise combinations from the 64 available breast cancer agents (Supplemental Table S1) examining which of them are currently used for therapy or in clinical trials. Of the potential 2,016 combinations, 170 are documented as tested by the ClinicalTrial.gov (26), the

FDA orange book, the NCI (http://www.cancer.gov/cancertopics/druginfo/breastcancer) or the DCDB (24). We considered these as clinically relevant combinations for breast cancer. The remaining ones constituted a set of non-tested combinations. Given the two sets, we computed the pathway crosstalk inhibition among the combined drugs. Since pathway crosstalk, as defined here, may only occur among related pathways sharing components, we only considered drug pairs whose pathways have at least a common protein, yielding a total of 1,132 combinations, 86 of which are among the 170 considered clinically relevant.

In general, we find that pathway pairs involved in clinically relevant combinations share a significantly higher portion of proteins and exhibit a higher crosstalk compared to a background of all human KEGG pathways (p-value < 2.2e-16; Supplemental Section S4 and Fig. S3). When specifically assessing the potential pathway crosstalk inhibition achieved by drug combinations, we observed that those in clinical use have a significantly higher impact on PCI than randomly combined pairs of drugs (Fig. 2A), with an average PCI of 0.34 compared to 0.25 (p-value = $8.96 \cdot 10^{-6}$). Indeed, for the few clinical drug combinations where efficacy data are available, we found that those

exceeding the average PCI of 0.34 are more likely to show clinical efficacy (p-value = 0.03215; Supplemental Section S5 and Fig. 2A and S4). This implies that crosstalk inhibition may be, one of the molecular mechanisms exploited by a number of successful breast cancer drug combinations.

In addition, we assessed the PCI for 68 synergistic, additive or antagonistic drug pairs identified in a combination screen performed in a tumor-derived liposarcoma cell line (DDLS817) considering 14 targeted compounds from distinct drug classes (16). This screen resulted in 14.3% synergistic, 38.5% additive and 22% antagonistic combinations. Figure 2B demonstrates that synergistic combinations have a significantly higher PCI than non-synergistic drug pairs and particularly antagonistic ones, with average values of 0.35 compared to 0.22 (p-value = 0.00341) and 0.18 (p-value = 0.00069), respectively. A significant correlation between PCI and drug combination index can be also observed as shown in Figure S5 (Pearson correlation coefficient = -0.439, p-value = 0.0001829). Furthermore, the average PCI of synergistic combinations is comparable to the one determined for clinically relevant combinations.

Overall, the two complementary evaluations support the value of our approach to identify effective drug combinations.

Identification of novel drug combinations

Among the randomly combined drugs, we found a large number of combinations showing a high impact on the crosstalk inhibition between breast cancer pathways (Fig. 2A and Supplemental Table S5). These drug pairs are promising candidates for combinatorial treatment since the pathway crosstalk identified is directly involved in breast cancer-related processes. To select the most relevant ones, we used as a threshold the mean PCI of 0.34 observed in the drug combination sets that are clinically used. This includes 62.8% of the clinically relevant combinations, exhibiting a higher likelihood of possessing clinical efficacy (Supplemental Fig. S4), but only 37.3% of the random set of combinations (Supplemental Fig. S6). Overall, 390 novel drug combinations showed a PCI ≥ 0.34, including drugs from 10 different classes, which are therefore likely to exhibit synergistic effects. Furthermore, pathway pairs affected by the novel drug combinations showed a significantly higher protein overlap as well as a higher pathway crosstalk compared to all human KEGG pathways with a p-value < 2.2e-16 (Supplemental Section S4 and Fig. S3). Not surprisingly, the majority of these combinations (370) occur between drugs belonging to different therapeutic subclasses, showing the ability of our method

to prevent redundant mechanisms of action. Moreover, about 65% of the new combinations include therapeutic classes never tested together before, expanding the sampling of the potential therapeutic space. We believe that these drug pairs have the potential to increase treatment efficacy by inhibiting oncogenic pathways at distinct points, as well as by reducing the concentration needed for inducing a given effect, which consequently improves their therapeutic index. A full description of the suggested drug combinations, together with the therapeutic pathways involved in the crosstalk inhibition, is provided in Supplemental Table S5.

Experimental validation of selected drug combinations

The fundamental aim of any combinatorial strategy is its therapeutic application. Therefore, we selected a subset of drug combinations to experimentally assess their effects on the proliferation of tumor cells, a key process for tumorigenesis. During the selection process, we only considered truly novel drug combinations; hence omitting those which resemble approved or tested ones (Supplemental Fig. S1). Trastuzumab, for instance, is administered in combination with paclitaxel and tamoxifen (32,33), thus we disregarded combinations including HER2 inhibitors together with microtubule or estrogen receptor modulators. We

selected ten combinations from the remaining pool according to their overall potential for crosstalk inhibition, involving ten targeted drugs and one cytotoxic agent (Fig. 3 and Table 1). To maximize the sampling of the combinatorial therapeutic space, we only selected the highest PCI per representative drug class combination.

We then studied the effect of the selected drug combinations in five human cancer cell lines, four of them representing distinct breast cancer subtypes (Fig. 4A), namely triple-negative (MDA-MB-231), hormone receptor-positive (MCF-7), HER2-overexpressing (SKBR3) and triple-positive (BT-474) breast cancer, while the fifth was derived from osteosarcoma (U2OS). For the quantification of cytotoxic effects induced by individual drugs or drug combinations, we used the MTT assay, which measures cell proliferation and viability (28) (Supplemental Section S1).

To determine if the tested combinations were of synergistic, additive or antagonistic nature, we computed the Loewe additivity-based drug combination index (DCI_X) for each combination in each cell line (30). The DCI_X compares the half-maximal effective concentrations for inhibiting X% of cell viability of single agents with the concentration derived for a combination. To avoid

overestimating the number of synergistic combinations and, to some extend, account for cell line variability, we adopted a more stringent definition of synergy (Supplemental Table S3), considering a DCI_X below 0.85 as synergistic. A DCI_X above 1.2 indicates antagonism while any value in-between depicts additivity ($0.85 > DCI_X \leq 1.2$) (29).

Considering an inhibition level of 50%, we generated sigmoid-fitted dose-response curves based on the MTT assays from which we then estimated IC_{50} and DCI_{50} values (Supplemental Fig. S2 for an example and S7 for all dose-response curves). Figure 4B shows the DCI_{50} derived for each combination in the five cell lines. Our results showed that seven out of ten combinations tested displayed a synergistic behavior in, at least, one cancer cell line. Overall, we found that 32% of the combinations were synergistic, 38% were additive, and 16% exhibited antagonistic effects in human cancer cell lines. For another 14% we could not determine a reliable DCI. Interestingly, the fraction of synergistic drug combinations slightly increased up to 35% when analyzing only breast cancer cell lines. These numbers emphasize the significant enrichment of synergistic drug combinations compared to traditional experimental high-throughput screens (p-value < 1e-04, Supplemental Fig. S8A and S8B), which

detect synergy in 4 to 14% of the drug pairs tested (16,34,35). A detailed description of the comparison can be found in the Supplementary Material (Section S6).

The per-combination perspective shows that the selected combinations are synergistic in a broader extent than anticipated *a priori* (Supplemental Fig. S9), given the heterogeneity of breast cancer (36,37). For instance, DC07 is synergistic in four cancer cell lines, DC04 and DC09 in three, DC02 and DC10 in two, and DC05 and DC06 in one.

When analyzing drug combinations separately, we observed clear correlations between the degree of synergy and the molecular features of each cancer cell line. In the case of DC09, trastuzumab combined with cabozantinib, a very strong synergy was identified in the HER2-overexpressing SKBR3 cells. Strong synergy was also observed for triple-positive cancer cells (BT-474), which express in addition to HER2, the estrogen and progesterone hormone receptors. Yet, in MCF-7 cells that lack HER2 overexpression, DC09 still showed some synergy, although decreased. In turn, complete lack of HER2 in the triple-negative and osteosarcoma cells revealed antagonistic interactions between trastuzumab and cabozantinib. The opposite trend was visible for DC10,

raloxifene and NVP-AEW541, which showed the best synergy in MCF-7 cells followed by BT-474 cells, while an additive effect was detected for SKBR3 cells. Surprisingly, a strong synergy was obtained for DC04 in MCF-7 cells and SKBR3 cells, although this combination includes a PARP1 inhibitor, which is expected to be effective in triple negative breast cancers (38). Note that, although individual breast cancer drug indications might give insights on the synergistic mechanisms of a combination in a certain cancer subtype (Supplemental Table S6), experiments in a larger cell panels would be required to elucidate the mechanism of synergy of a combinations regarding a certain cancer subtype.

When considering the combinatorial effects with respect to the individual cancer cell lines, we observed that MCF-7 cells and SKBR3 cells tend to be more sensitive towards the selected drug combinations, with 50% being synergistic and the remaining ones showing at least additive effects (Supplemental Fig. S10). Again, this enrichment is significant with respect to high-throughput screens (p-value = 5e-04, Supplemental Fig. S8C). In turn, 30% of the combinations were antagonistic in U2OS cells and BT-474 cells, and 20% were antagonistic in MDA-MB-231 cells. These observations might reflect the prevalence of therapeutic strategies, i.e., drugs and combinations, for the more

common hormone receptor-positive and HER2-overexpressing breast cancer subtypes.

U2OS cells were included as additional cancer cell line to examine the specificity of synergistic effects, since we recently found that individual anti-cancer drugs designed for a particular cancer (sub)type do not show a significantly higher activity in cancer cell lines derived from that specific tumor type (39).

Although the IC_{50} is the most used index to measure the effectiveness of a compound at inhibiting a specific biological function, we examined the potential effect of concentration-dependent pharmacodynamic interactions, we determined the DCI for a series of inhibition levels ranging from 20% to 80%, which corresponds to DCI_{20} to DCI_{80}. Overall, we found our results to be fairly robust, with 68.3% of the combinations showing a consistent interaction behavior, independently of the inhibition level considered - i.e. we found neither synergistic-antagonistic nor additive-antagonistic shifts (Supplemental Fig. S11A).

Effect of the raloxifene and cabozantinib combination in a xenograft mouse model

The experimental validation in cancer cell lines revealed a clear synergistic therapeutic effect for combination DC02 (raloxifene with cabozantinib) in hormone receptor-positive breast cancer cells (DCI_{50} = 0.39). Our computational model suggested that the observed crosstalk inhibition was the result of the simultaneous modulation of estrogen signaling together with the PI3K/AKT and VEGF pathways by the two drugs, which should not only reduce the growth of the primary tumor but also its ability to spread. Interestingly, we found that this particular combination exhibited a dose reduction index of 51.9 and 2.66 for raloxifene and cabozantinib, respectively. In other words, to achieve the same inhibition level, the doses of the individual drugs could be significantly reduced when combined (Fig. 5). Finally, its DCI showed a remarkably consistent synergistic behavior in MCF-7 cells throughout all the inhibition levels (Supplemental Fig. S11B).

We thus examined the impact of DC02 *in vivo*, using MCF-7 cells orthotopically implanted in nude mice, which were treated for 15 days with cabozantinib, raloxifene or the combination of both. We selected concentrations of 1 mg/kg

for cabozantinib and 3 mg/kg for raloxifene (low doses) that were previously reported to have a minor or no effect on tumor growth in related conditions (40,41). However, since mice treated with the combination were exposed to higher overall drug doses, we assessed the effect of the individual drugs on tumor growth doubling their concentrations. Thus, we applied 2 mg/kg for cabozantinib and 6 mg/kg for raloxifene to avoid that a stronger effect observed for the combination is merely induced by the higher drug concentration administered in the combinatorial treatment.

We found that treating tumor-bearing mice with cabozantinib or raloxifene alone induced a cytostatic effect on tumor growth (Fig. 6A). Strikingly, in agreement with our observations in cultured cell lines and the crosstalk inhibition model, the combined treatment of mice with lower doses of cabozantinib and raloxifene showed a clear synergistic effect reducing the size of the tumors by more than 60% (Fig. 6A). Despite its dramatic impact on tumor growth, the combination has no effect on the body weight and none of the animals demonstrated abnormalities in their behavior, indicating that the combinatorial treatment is not more stressful than individual treatments (Supplemental Fig. S12). To explore whether the molecular processes leading to

tumor reduction were indeed the ones suggested by the crosstalk inhibition model, we performed immunohistochemical analyses of tumor sections at the end of the treatment (day 15). TUNEL staining assays showed slightly increased cell death levels in tumors from cabozantinib-treated mice but no differences in the raloxifene-treated mice, which is consistent with observations in ER^+ human breast tumors (42). Interestingly, when combining both drugs, cell death levels increased 9.5 times compared with the initial or vehicle-treated tumors (Fig. 6B and 6C). We also found that cell proliferation, based on Ki67 staining, was strongly inhibited in tumors from mice treated with raloxifene and, to an even larger extent, in tumors from mice treated with the combined drugs (Fig. 6D). We did not observe any effect on cell proliferation in tumors from cabozantinib-treated mice.

The effects on cell proliferation and cell death, as detected in the xenograft mouse tumors, were in line with the current knowledge on the mechanism of action of both drugs (40,42-44). To further assess pathway crosstalk inhibition for DC02 at the molecular level, we performed western blotting with tumor samples. In particular, we analyzed the activity of proteins involved in the pathways that were predicted to be modulated predominantly by the drug

combination, including Akt and Src and the nuclear form of the estrogen receptor (nER) (Fig. 6E). We found that the drug combination had a stronger effect than the individual drugs on the activities of both Src and Akt, which was also clear analyzing downstream members of the pathways such as Bcl2 and cyclin D1 (Fig. 6F). These results are consistent with the proposed effect of the drug combination on crosstalk signaling and the reduced tumor growth observed in the xenografts.

Taken together, our study confirms that the combination of cabozantinib and raloxifene has a stronger therapeutic effect *in vivo* than the single drugs at higher doses. Our results indicate that the dramatic, synergistic effect of the combination on tumor growth emerges from the simultaneous induction of cell death by cabozantinib and the inhibition of cell proliferation by raloxifene. These mechanistic insights agree with the crosstalk inhibition calculated for DC02, which mostly comes from the simultaneous modulation of estrogen and prolactin signaling together with the PI3K/AKT and VEGF signaling pathways by the two drugs. Thus, as suggested by our model, inhibiting the crosstalk between these pathways prevents alternative signaling events, which regulate cell proliferation and survival.

Discussion

Combinatorial therapy is a very promising strategy for improving cancer treatment. The combination of drugs allow to interfere with compensatory mechanisms, often related to treatment failure, using drug concentrations that are less toxic than the high doses of single drugs usually required to achieve similar effects. However, despite its great potential, most approved drug combinations are the result of empirical clinical experience and, not being rationally designed, cover only a small fraction of the vast therapeutic space. In this study, we have presented a computational network biology approach to identify potentially synergistic drug combinations against breast cancer. Even though we focus specifically on pathway crosstalk as a major contributor to treatment failure, other oncogenic features, such as gene mutations, might also be helpful for finding combinatorial treatment (45). Overall, our strategy has identified a set of anti-cancer drug pairs with a large impact on crosstalk inhibition. The experimental validation of ten selected novel combinations confirmed a synergistic behavior for seven of them in, at least, one of the four breast cancer cell lines tested. This represents a significant enrichment compared to combinatorial studies without computational prioritization.

Furthermore, we confirmed that raloxifene combined with cabozantinib has a dramatic synergistic effect interfering with tumor growth *in vivo* using a mouse xenograft model based on MCF-7 human breast cancer cells, supporting the potential clinical relevance of our strategy. Even though further research is required to enable the translation of a promising combination into therapeutic strategies, our results show that approaches focusing on the inhibition of crosstalk between pathways could provide valuable mechanistic information to discover synergistic drug effects. Moreover, we centered our study on breast cancer, but we believe that our approach can be also applied to other complex diseases, in which pathway crosstalk is likely to play an important role.

Acknowledgements

We would like to thank Miquel Duran-Frigola (IRB Barcelona) for extensive and critical discussions.

References

1. Polyak K. Heterogeneity in breast cancer. J Clin Invest 2011;121:3786-8.
2. Geyer FC, Weigelt B, Natrajan R, Lambros MB, de Biase D, Vatcheva R, et al. Molecular analysis reveals a genetic basis for the phenotypic diversity of metaplastic breast carcinomas. J Pathol 2010;220:562-73.
3. Gibbs JB. Mechanism-based target identification and drug discovery in cancer research. Science 2000;287:1969-73.
4. Mills GB. An emerging toolkit for targeted cancer therapies. Genome Res 2012;22:177-82.
5. Osborne CK, Schiff R. Mechanisms of endocrine resistance in breast cancer. Annu Rev Med 2011;62:233-47.
6. Tsang RY, Finn RS. Beyond trastuzumab: novel therapeutic strategies in HER2-positive metastatic breast cancer. Br J Cancer 2012;106:6-13.
7. Al-Lazikani B, Banerji U, Workman P. Combinatorial drug therapy for cancer in the post-genomic era. Nat Biotechnol 2012;30:679-92.
8. Higgins MJ, Baselga J. Targeted therapies for breast cancer. J Clin Invest 2011;121:3797-803.
9. Lehar J, Krueger AS, Avery W, Heilbut AM, Johansen LM, Price ER, et al. Synergistic drug combinations tend to improve therapeutically relevant selectivity. Nat Biotechnol 2009;27:659-66.
10. Iadevaia S, Lu Y, Morales FC, Mills GB, Ram PT. Identification of optimal drug combinations targeting cellular networks: integrating phospho-proteomics and computational network analysis. Cancer research 2010;70:6704-14.
11. Wong PK, Yu F, Shahangian A, Cheng G, Sun R, Ho CM. Closed-loop control of cellular functions using combinatory drugs guided by a stochastic search algorithm. Proceedings of the National Academy of Sciences of the United States of America 2008;105:5105-10.
12. Lebedeva G, Sorokin A, Faratian D, Mullen P, Goltsov A, Langdon SP, et al. Model-based global sensitivity analysis as applied to identification of anti-cancer drug targets and biomarkers of drug resistance in the ErbB2/3 network. European journal of pharmaceutical sciences : official journal of the European Federation for Pharmaceutical Sciences 2012;46:244-58.
13. Havaleshko DM, Cho H, Conaway M, Owens CR, Hampton G, Lee JK, et al. Prediction of drug combination chemosensitivity in human bladder cancer. Molecular cancer therapeutics 2007;6:578-86.
14. Tang J, Karhinen L, Xu T, Szwajda A, Yadav B, Wennerberg K, et al. Target inhibition networks: predicting selective combinations of druggable targets to block cancer survival pathways. PLoS Comput Biol 2013;9:e1003226.

15. Tang J, Aittokallio T. Network pharmacology strategies toward multi-target anticancer therapies: from computational models to experimental design principles. Current pharmaceutical design 2014;20:23-36.
16. Miller ML, Molinelli EJ, Nair JS, Sheikh T, Samy R, Jing X, et al. Drug synergy screen and network modeling in dedifferentiated liposarcoma identifies CDK4 and IGF1R as synergistic drug targets. Sci Signal 2013;6:ra85.
17. Bernards R. A missing link in genotype-directed cancer therapy. Cell 2012;151:465-8.
18. Yamaguchi H, Chang SS, Hsu JL, Hung MC. Signaling cross-talk in the resistance to HER family receptor targeted therapy. Oncogene 2013.
19. Hopkins AL. Network pharmacology: the next paradigm in drug discovery. Nat Chem Biol 2008;4:682-90.
20. Jaeger S, Aloy P. From protein interaction networks to novel therapeutic strategies. IUBMB Life 2012;64:529-37.
21. Knox C, Law V, Jewison T, Liu P, Ly S, Frolkis A, et al. DrugBank 3.0: a comprehensive resource for 'omics' research on drugs. Nucleic Acids Res 2011;39:D1035-41.
22. Zhu F, Shi Z, Qin C, Tao L, Liu X, Xu F, et al. Therapeutic target database update 2012: a resource for facilitating target-oriented drug discovery. Nucleic Acids Res 2012;40:D1128-36.
23. Kanehisa M, Goto S, Sato Y, Furumichi M, Tanabe M. KEGG for integration and interpretation of large-scale molecular data sets. Nucleic Acids Res 2012;40:D109-14.
24. Liu Y, Hu B, Fu C, Chen X. DCDB: drug combination database. Bioinformatics 2010;26:587-8.
25. Hare D, Foster T. The Orange Book: the Food and Drug Administration's advice on therapeutic equivalence. Am Pharm 1990;NS30:35-7.
26. Zarin DA, Tse T, Williams RJ, Califf RM, Ide NC. The ClinicalTrials.gov results database--update and key issues. N Engl J Med 2011;364:852-60.
27. Csermely P, Agoston V, Pongor S. The efficiency of multi-target drugs: the network approach might help drug design. Trends Pharmacol Sci 2005;26:178-82.
28. van Meerloo J, Kaspers GJ, Cloos J. Cell sensitivity assays: the MTT assay. Methods Mol Biol 2011;731:237-45.
29. Chou TC. Theoretical basis, experimental design, and computerized simulation of synergism and antagonism in drug combination studies. Pharmacological reviews 2006;58:621-81.
30. Chou TC, Talalay P. Quantitative analysis of dose-effect relationships: the combined effects of multiple drugs or enzyme inhibitors. Adv Enzyme Regul 1984;22:27-55.

31. Ritz C, Streibig JC. Bioassay analysis using R. Journal of Statistical Software 2005;12.
32. Slamon DJ, Leyland-Jones B, Shak S, Fuchs H, Paton V, Bajamonde A, et al. Use of chemotherapy plus a monoclonal antibody against HER2 for metastatic breast cancer that overexpresses HER2. N Engl J Med 2001;344:783-92.
33. Jones A. Combining trastuzumab (Herceptin) with hormonal therapy in breast cancer: what can be expected and why? Annals of oncology : official journal of the European Society for Medical Oncology / ESMO 2003;14:1697-704.
34. Borisy AA, Elliott PJ, Hurst NW, Lee MS, Lehar J, Price ER, et al. Systematic discovery of multicomponent therapeutics. Proceedings of the National Academy of Sciences of the United States of America 2003;100:7977-82.
35. Zhang L, Yan K, Zhang Y, Huang R, Bian J, Zheng C, et al. High-throughput synergy screening identifies microbial metabolites as combination agents for the treatment of fungal infections. Proceedings of the National Academy of Sciences of the United States of America 2007;104:4606-11.
36. van 't Veer LJ, Dai H, van de Vijver MJ, He YD, Hart AA, Mao M, et al. Gene expression profiling predicts clinical outcome of breast cancer. Nature 2002;415:530-6.
37. Perou CM, Sorlie T, Eisen MB, van de Rijn M, Jeffrey SS, Rees CA, et al. Molecular portraits of human breast tumours. Nature 2000;406:747-52.
38. Dent RA, Lindeman GJ, Clemons M, Wildiers H, Chan A, McCarthy NJ, et al. Phase I trial of the oral PARP inhibitor olaparib in combination with paclitaxel for first- or second-line treatment of patients with metastatic triple-negative breast cancer. Breast cancer research : BCR 2013;15:R88.
39. Jaeger S, Duran-Frigola M, Aloy P. Drug sensitivity in cancer cell lines is not tissue-specific. Molecular cancer 2015;14:312.
40. Yakes FM, Chen J, Tan J, Yamaguchi K, Shi Y, Yu P, et al. Cabozantinib (XL184), a novel MET and VEGFR2 inhibitor, simultaneously suppresses metastasis, angiogenesis, and tumor growth. Molecular cancer therapeutics 2011;10:2298-308.
41. Brady H, Desai S, Gayo-Fung LM, Khammungkhune S, McKie JA, O'Leary E, et al. Effects of SP500263, a novel, potent antiestrogen, on breast cancer cells and in xenograft models. Cancer research 2002;62:1439-42.
42. Dowsett M, Bundred NJ, Decensi A, Sainsbury RC, Lu Y, Hills MJ, et al. Effect of raloxifene on breast cancer cell Ki67 and apoptosis: a double-blind, placebo-controlled, randomized clinical trial in postmenopausal patients. Cancer epidemiology, biomarkers & prevention : a publication of the American Association for Cancer Research, cosponsored by the American Society of Preventive Oncology 2001;10:961-6.

43. Kurzrock R, Sherman SI, Ball DW, Forastiere AA, Cohen RB, Mehra R, et al. Activity of XL184 (Cabozantinib), an oral tyrosine kinase inhibitor, in patients with medullary thyroid cancer. J Clin Oncol 2011;29:2660-6.
44. Martin LA, Dowsett M. BCL-2: a new therapeutic target in estrogen receptor-positive breast cancer? Cancer cell 2013;24:7-9.
45. Sun C, Hobor S, Bertotti A, Zecchin D, Huang S, Galimi F, et al. Intrinsic resistance to MEK inhibition in KRAS mutant lung and colon cancer through transcriptional induction of ERBB3. Cell reports 2014;7:86-93.

Tables

Table 1: List of drug combinations selected for experimental validation. For each combination, we specified the respective drug classes as well as the overall pathway crosstalk inhibition (PCI). (SERM – selective estrogen receptor modulator)

Combination	Drug1	Drug class	Drug2	Drug class	PCI
DC01	Cabozantinib	VEGFR inhibitor	Erlotinib	EGFR inhibitor	0.60
DC02	Cabozantinib	VEGFR inhibitor	Raloxifene	SERM	0.50
DC03	Olaparib	PARP-1 inhibitor	Tanespimycin	HSP inhibitor	0.88
DC04	Olaparib	PARP-1 inhibitor	Dinaciclib	CDK inhibitor	1.0
DC05	Olaparib	PARP-1 inhibitor	PD-0332991	CDK inhibitor	0.72
DC06	Cabozantinib	VEGFR inhibitor	PD-0332991	CDK inhibitor	0.34
DC07	Paclitaxel	Microtubule modulator	Tanespimycin	HSP inhibitor	0.38
DC08	Paclitaxel	Microtubule modulator	Midostaurin	VEGFR inhibitor	0.44

DC09	Cabozantinib	VEGFR inhibitor	Trastuzumab	HER2 inhibitor	0.57
DC10	Figitumumab	IGF-1R inhibitor	Raloxifene	SERM	0.80

Figure legends

Figure 1. Pathway crosstalk inhibition.

A. Crosstalk identified between pathways A and B, defined as shared protein interactions, or those occurring downstream of them, in the individual pathways. The flow of information within the crosstalk network, i.e., the network efficiency, is 0.29. **B.** Drug 1 inhibits signaling through pathway A but does not affect

crosstalk inhibition. In consequence, proliferation is not effectively inhibited. **C.** Drug 2 reduces signaling through the crosstalk network to 0.05, resulting in a pathway crosstalk inhibition of 0.83. **D.** Crosstalk signaling is completely prevented by using D1 and D2 in combination.

Figure 2. *In silico* validation of the pathway crosstalk inhibition (PCI) index.

A. Comparison of the PCI distributions for the populations of clinically relevant breast cancer drug combinations (i.e. currently in use or in clinical trials) and randomly combined breast cancer drugs (p-value = 8.96×10^{-6}) as well as for combinations with and without confirmed clinical benefit (p-value = 0.03215). B. Evaluation of the PCI of 13 synergistic combinations with 55 non-synergistic (p-value = 0.00341), 35 additive (p-value = 0.01667) and 20 antagonistic (p-value = 0.00069) drug pairs identified among 14 targeted compounds within a liposarcoma cell line (16). P-value legend: * $p < 0.05$, ** $p < 0.01$, *** $p < 0.001$, **** $p < 0.0001$.

Figure 3. Pathway crosstalk inhibition between pairs of breast cancer therapeutics, both approved and experimental.

Drug combinations in use are indicated with a black dot. Combinations selected for experimental validation are marked with a red star (see also Table 1). Drugs are colored according to their therapeutic classes. Drugs not involved in any pathway crosstalk or its inhibition were removed for better illustration. Note that drugs belonging to the same class might still target different sets of proteins, and thus the crosstalk inhibition achieved when combined with other drugs might vary.

Figure 4. Effect of different drug combinations on selected human cancer cell lines.

A. Overview of the main molecular characteristics of the four breast cancer cell lines (in gray) and the osteosarcoma cell line (U2OS). **B.** Experimental DCI values derived for each combination and cell line at an inhibition level of 50%. A DCI_{50} of zero depicts drug combinations in which none of the single agents yields an IC_{50} but the combination does. Blank cells indicate combinations for which no dose-response curves could be modeled (3 cases) or in which neither the single nor the dual perturbation reached the IC_{50} (5 cases). The histogram shows the distribution of DCI_{50} values for breast cancer cell lines only.

Figure 5. Pharmacodynamic interaction between raloxifene and cabozantinib.

Isobologram showing the interaction behavior between raloxifene and cabozantinib. Blue and green symbols denote the IC_{50} of raloxifene and cabozantinib, respectively, while the red symbol represents the combination. The dotted line indicates additivity. Data points below this line display synergy, while points above imply antagonism. The dose reduction index (DRI) exhibits to which extent the concentration of a drug in combination can be reduced at a given inhibition level compared to the single concentrations.

Figure 6. Effect of raloxifene, cabozantinib and combinatorial treatment on tumor growth in a MCF-7 xenograft model.

A. Athymic nude mice, orthotopically injected with $1x10^6$ MCF-7 cells, were treated for 15 days with cabozantinib (2 mg/kg), raloxifene (6 mg/kg), the combination of cabozantinib (1 mg/kg) and raloxifene (3 mg/kg), or vehicle. Single treatments were combined with the corresponding vehicle of the other drug. Tumor size was measured at the indicated times and was normalized according to the original size of each tumor at the start of the treatment. Nine mice with two tumors each were used per condition B. Representative TUNEL

staining of tumors collected at day 15. Significant increases in cell death levels were measured for cabozantinib (p-value = 0.0015) and the combination (p-value = 0.00016) compared to vehicle. **C.** Average area of positive TUNEL-stained cells quantified by ImageJ for each treatment. **D.** Representative H&E and Ki67 staining of the initial tumor, vehicle, cabozantinib and raloxifene alone, and the combination of both at day 15. Images shown are 20X. The percentage of positive Ki67-stained cells is indicated below each group. **E.** Visualization of the simplified crosstalk network between the estrogen and the VEGFR signaling pathway for DC02. Proteins analyzed by Western Blot (WB) are colored from yellow to blue. **F.** Western blot analysis of phospho-Akt, phospho-Src, Bcl-2 and Cyclin D1 to assess their activity with respect to pathway crosstalk inhibition. Tubulin was used as a loading control.

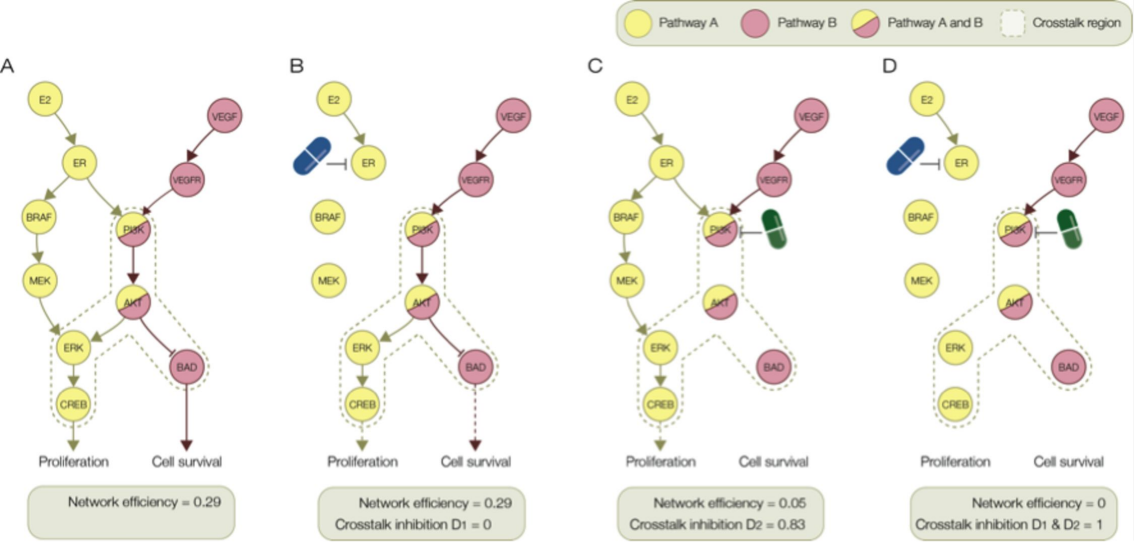
Pathway A
Pathway B
Pathway A and B
Crosstalk region
A
B
C
D
E2
VEGF
ER
VEGFR
BRAF
PI3K
MEK
AKT
ERK
BAD
CREB
Proliferation
Cell survival
Network efficiency = 0.29
Network efficiency = 0.29
Crosstalk inhibition D1 = 0
Network efficiency = 0.05
Crosstalk inhibition D2 = 0.83
Network efficiency = 0
Crosstalk inhibition D1 & D2 = 1

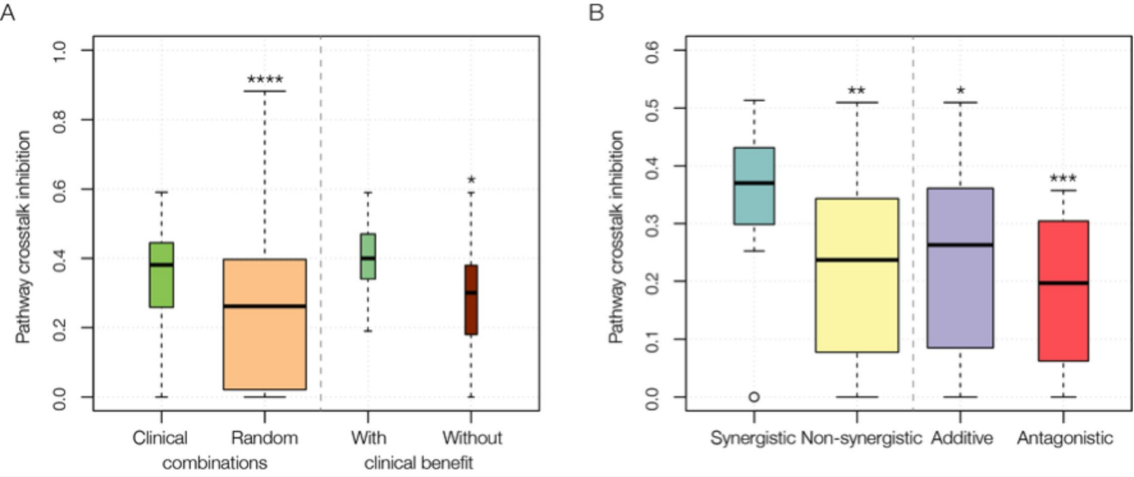
A
Pathway crosstalk inhibition
0.0
0.2
0.4
0.6
0.8
1.0
****
*
Clinical combinations
Random
With clinical benefit
Without
B
Pathway crosstalk inhibition
0.0
0.1
0.2
0.3
0.4
0.5
0.6
**
*
***
Synergistic
Non-synergistic
Additive
Antagonistic

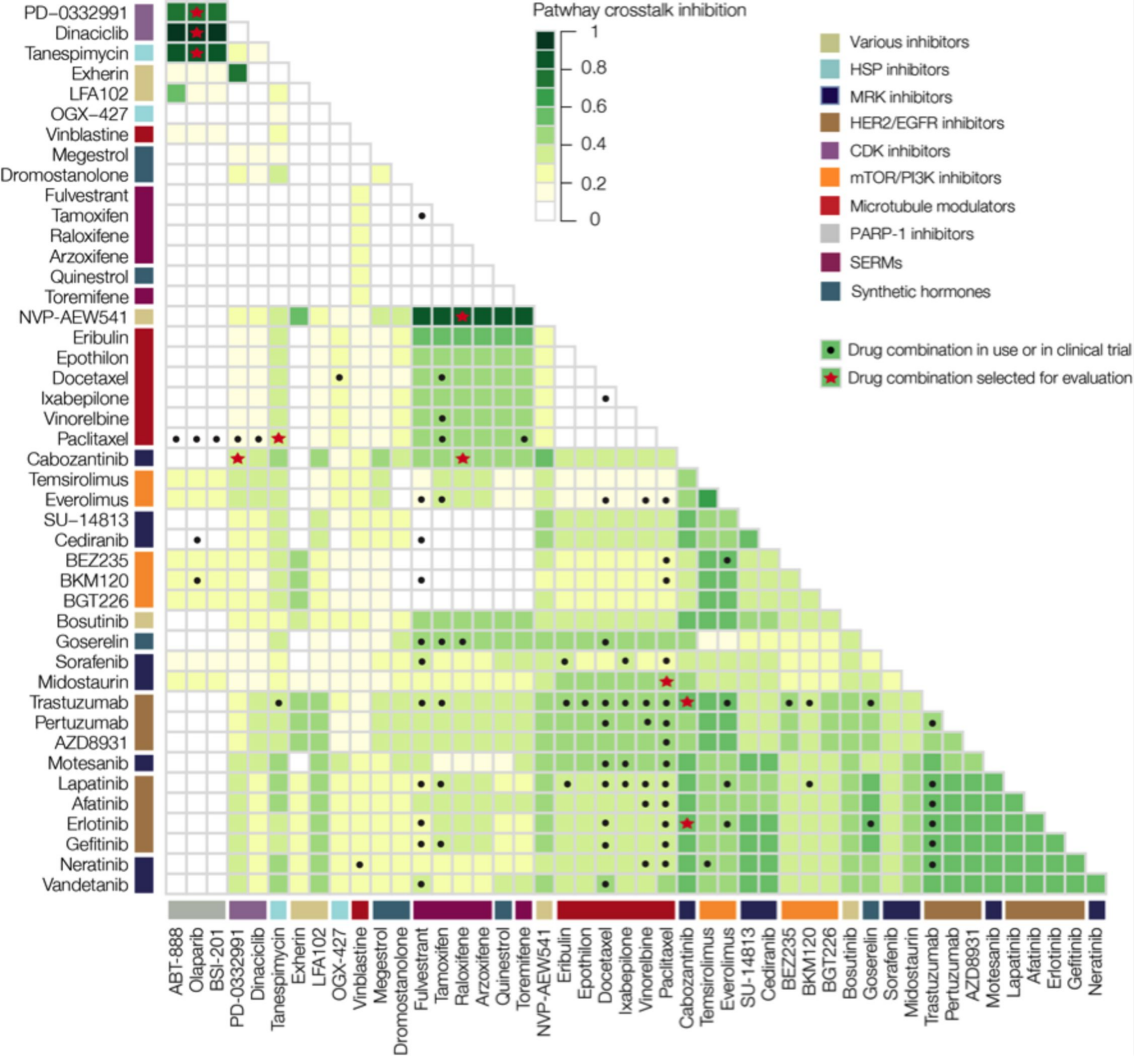
Patwhay crosstalk inhibition
1
0.8
0.6
0.4
0.2
0
Various inhibitors
HSP inhibitors
MRK inhibitors
HER2/EGFR inhibitors
CDK inhibitors
mTOR/PI3K inhibitors
Microtubule modulators
PARP-1 inhibitors
SERMs
Synthetic hormones
Drug combination in use or in clinical trial
Drug combination selected for evaluation
PD−0332991
Dinaciclib
Tanespimycin
Exherin
LFA102
OGX−427
Vinblastine
Megestrol
Dromostanolone
Fulvestrant
Tamoxifen
Raloxifene
Arzoxifene
Quinestrol
Toremifene
NVP-AEW541
Eribulin
Epothilon
Docetaxel
Ixabepilone
Vinorelbine
Paclitaxel
Cabozantinib
Temsirolimus
Everolimus
SU−14813
Cediranib
BEZ235
BKM120
BGT226
Bosutinib
Goserelin
Sorafenib
Midostaurin
Trastuzumab
Pertuzumab
AZD8931
Motesanib
Lapatinib
Afatinib
Erlotinib
Gefitinib
Neratinib
Vandetanib
ABT-888
Olaparib
BSI-201
PD-0332991
Dinaciclib
Tanespimycin
Exherin
LFA102
OGX-427
Vinblastine
Megestrol
Dromostanolone
Fulvestrant
Tamoxifen
Raloxifene
Arzoxifene
Quinestrol
Toremifene
NVP-AEW541
Eribulin
Epothilon
Docetaxel
Ixabepilone
Vinorelbine
Paclitaxel
Cabozantinib
Temsirolimus
Everolimus
SU-14813
Cediranib
BEZ235
BKM120
BGT226
Bosutinib
Goserelin
Sorafenib
Midostaurin
Trastuzumab
Pertuzumab
AZD8931
Motesanib
Lapatinib
Afatinib
Erlotinib
Gefitinib
Neratinib

A

	MDA-MB-231	MCF-7	SKBR3	BT-474	U2OS
Luminal	○	⊕	⊕	⊕	Osteosarcoma
Basal	⊕	○	○	○	
ER	○	⊕	○	⊕	
PR	○	⊕	○	⊕	
HER2	○	○	⊕	⊕	
Known mutations	BRAF CDKN2A KRAS NF2 TP53	CDKN2A PI3KCA	TP53	PI3KCA TP53	CDKN2A
Histology Subtype	Metastatic Adeno-carcinoma	Metastatic Adeno-carcinoma	Adeno-carcinoma	Invasive ductal carcinoma	Sarcoma of the tibia

B

	MDA-MB-231	MCF-7	SKBR3	BT-474	U2OS
DC01	0.91	0.98	1.08	1.15	0.86
DC02	0.98	0.39	0.64	1.35	1.41
DC03		1.18	1.10	1.07	0.89
DC04	0.88	0.70	0.72	1.03	0.84
DC05	0.76	1.04			1.33
DC06	0.91	1.01	0.84	1.25	0.93
DC07	0.64	0.67	0.78	2.12	0.25
DC08	70.27				
DC09	1.36	0.66	0	0.37	3.40
DC10	0.88	0.68	1.00	0.84	1.10

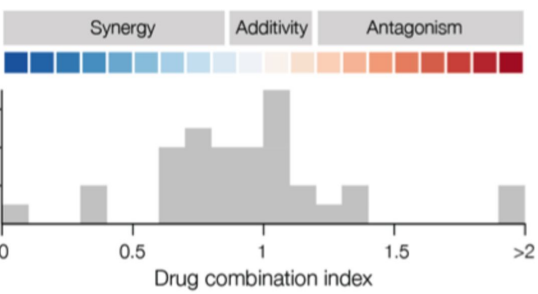

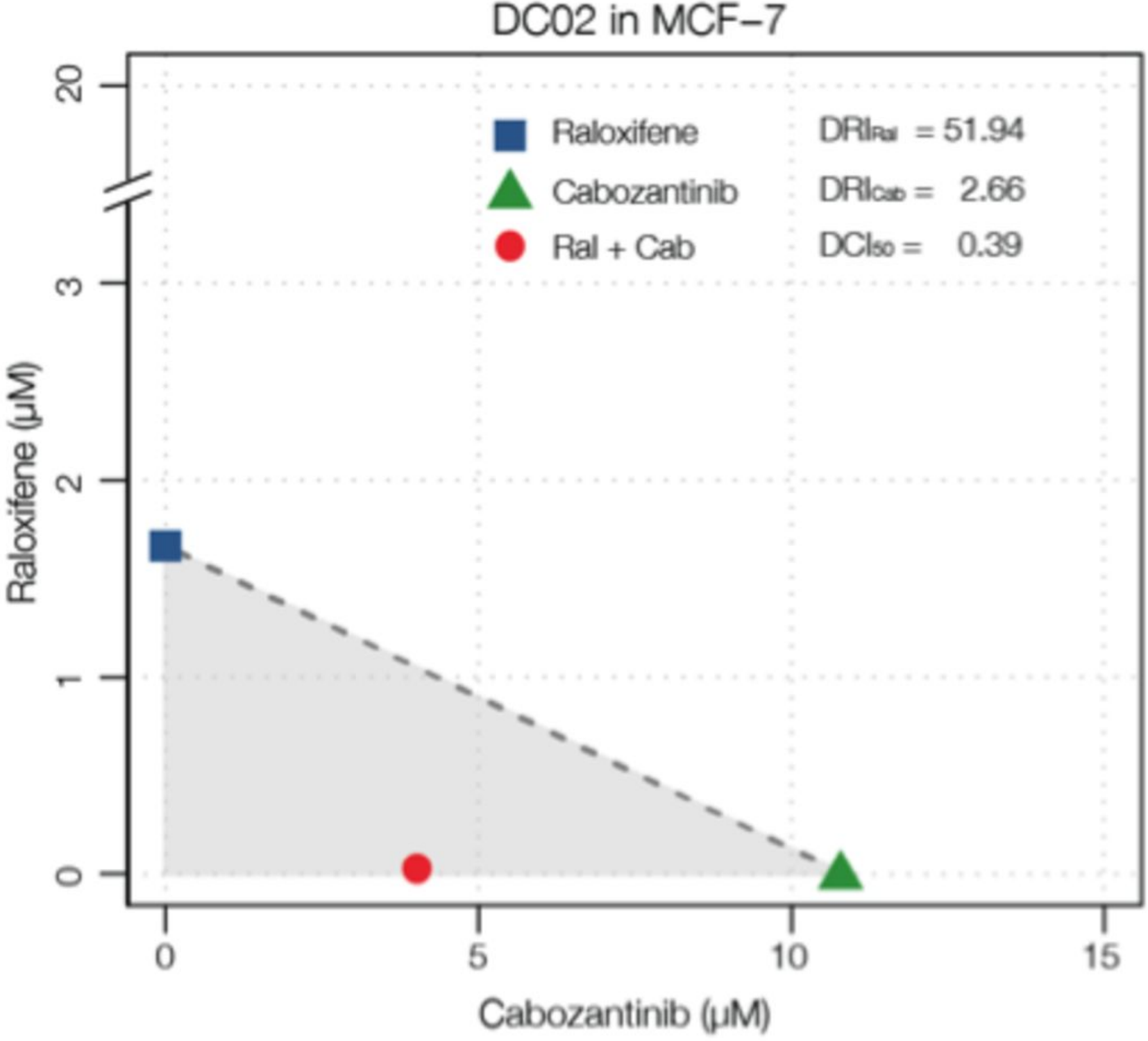
DC02 in MCF−7
Raloxifene
Cabozantinib
Ral + Cab
DRIRal = 51.94
DRICab = 2.66
DCIS0 = 0.39
Raloxifene (μM)
Cabozantinib (μM)
0
1
2
3
20
0
5
10
15

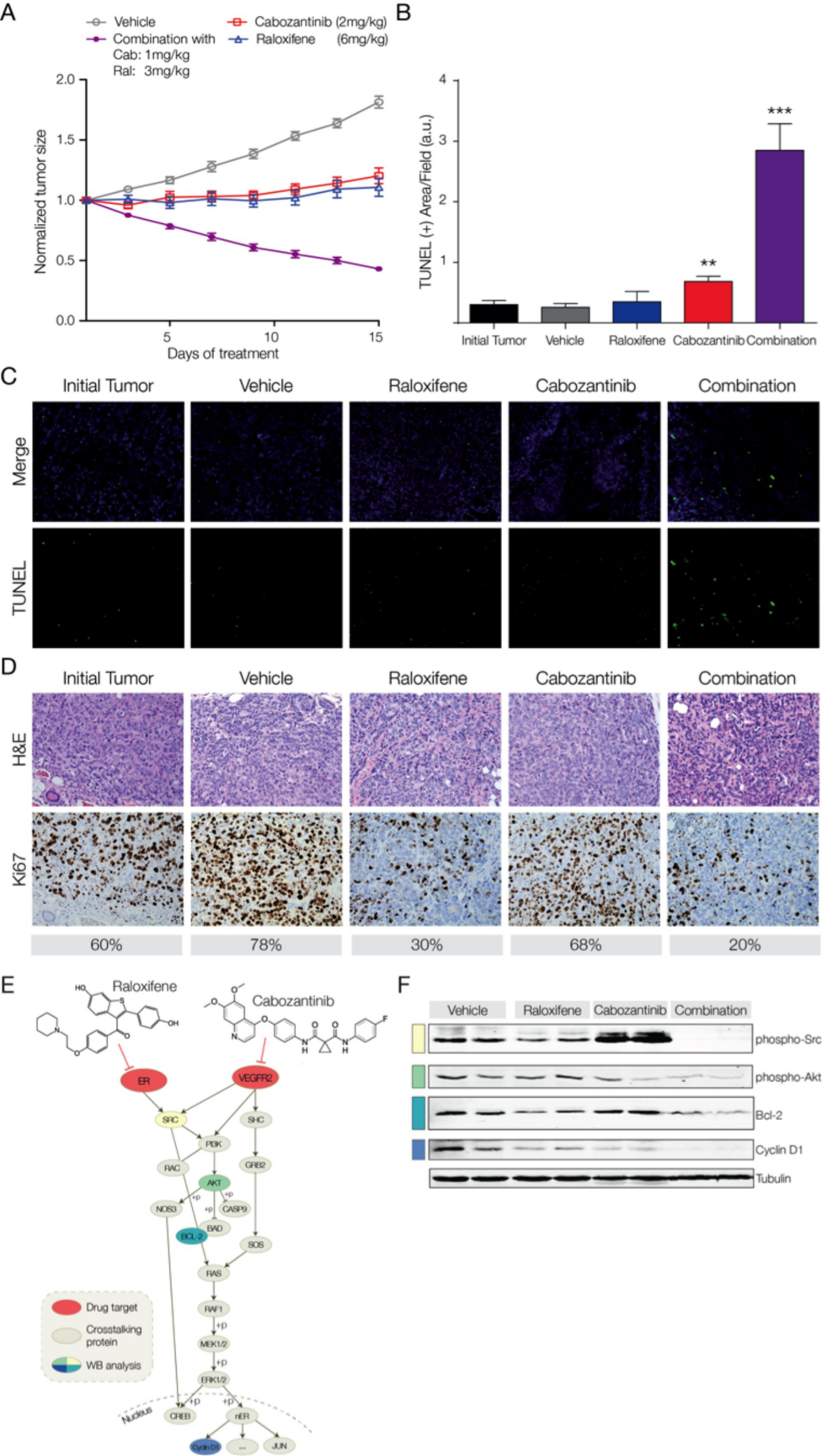
A
Vehicle
Combination with Cab: 1mg/kg Ral: 3mg/kg
Cabozantinib (2mg/kg)
Raloxifene (6mg/kg)
Normalized tumor size
Days of treatment
B
TUNEL (+) Area/Field (a.u.)
**
***
Initial Tumor
Vehicle
Raloxifene
Cabozantinib
Combination
C
Initial Tumor
Vehicle
Raloxifene
Cabozantinib
Combination
Merge
TUNEL
D
Initial Tumor
Vehicle
Raloxifene
Cabozantinib
Combination
H&E
Ki67
60%
78%
30%
68%
20%
E
Raloxifene
Cabozantinib
ER
VEGFR2
SRC
SHC
PI3K
RAC
GRB2
AKT
NOS3
CASP9
BAD
BCL-2
SOS
RAS
RAF1
MEK1/2
ERK1/2
Nucleus
CREB
nER
JUN
Drug target
Crosstalking protein
WB analysis
F
Vehicle
Raloxifene
Cabozantinib
Combination
phospho-Src
phospho-Akt
Bcl-2
Cyclin D1
Tubulin